tvst

Retina

Retinal Pigment Epithelium and Outer Retinal Atrophy (RORA) in Retinitis Pigmentosa: Functional, Structural, and Genetic Evaluation

Maria Cristina Savastano[1,2,*], Giorgio Placidi[1,2,*], Claudia Fossataro[1,2], Federico Giannuzzi[1,2,#], Nicola Claudio D'Onofrio[1,2], Lorenzo Hu[1,2], Valentina Cestrone[1,2], Elena D'Agostino[1,2], Ilaria Biagini[1–3], Ludovica Paris[1,2], Giorgia Coppa[1,2], Clara Rizzo[4], Raphael Kilian[5], Pietro Chiurazzi[6,7], Matteo Bertelli[8,9], Paolo Enrico Maltese[8], Benedetto Falsini[1,2], and Stanislao Rizzo[1,2]

[1] Ophthalmology Unit, Fondazione Policlinico Universitario Agostino Gemelli IRCCS, Rome, Italy
[2] Università Cattolica del Sacro Cuore, Rome, Italy
[3] Department of Neurosciences, Psychology, Drug Research and Child Health (NEUROFARBA), University of Florence and AOU Careggi, Firenze, Italy
[4] Ophthalmology, Department of Surgical, Medical and Molecular Pathology and Critical Care Medicine, University of Pisa, Pisa, Italy
[5] Ophthalmology Unit, University of Verona, Verona, Italy
[6] Medical Genetics, Fondazione Policlinico Universitario Agostino Gemelli IRCCS, Rome, Italy
[7] Genomic Medicine, Università Cattolica del Sacro Cuore, Rome, Italy
[8] Magi's Lab, Rovereto, Italy.
[9] Magi Euregio, Bolzano, Italy

Correspondence: Federico Giannuzzi, Ophthalmology Unit, Fondazione Policlinico Universitario Agostino Gemelli IRCCS, Largo A. Gemelli, 8, Rome 00136, Italy. e-mail: federico.giannuzzi@gmail.com

Received: August 31, 2023
Accepted: July 14, 2024
Published: August 30, 2024

Keywords: retinal degeneration; retinitis pigmentosa; disease staging; multimodal imaging; OCT; subretinal illumination; electroretinography; RORA

Citation: Savastano MC, Placidi G, Fossataro C, Giannuzzi F, D'Onofrio NC, Hu L, Cestrone V, D'Agostino E, Biagini I, Paris L, Coppa G, Rizzo C, Kilian R, Chiurazzi P, Bertelli M, Maltese PE, Falsini B, Rizzo S. Retinal pigment epithelium and outer retinal atrophy (RORA) in retinitis pigmentosa: Functional, structural, and genetic evaluation. Transl Vis Sci Technol. 2024;13(8):44, https://doi.org/10.1167/tvst.13.8.44

Purpose: To examine whether the extension of retinal pigment epithelium (RPE) and outer retinal atrophy (RORA) and various other morphofunctional parameters correlate with the genetic assessment and severity of retinitis pigmentosa (RP).

Methods: Thirty-eight patients (76 eyes) with RP were prospectively enrolled and underwent full ophthalmic examination, including visual field testing, full-field electroretinography (ERG), and optical coherence tomography angiography. The severity of the disease was calculated using the RP stage scoring system, and the area of RORA was assessed using the automatically calculated area of sub-RPE illumination. Blood or saliva samples were collected from subjects, and DNA extraction was performed to evaluate genetic mutations and nucleotide and amino acid variations.

Results: There was a statistically significant correlation between the extent of RORA and patient age, best-corrected visual acuity, ellipsoid zone extension, and disease severity in both eyes (each, $P < 0.05$). In contrast, RORA did not correlate with either the visual field or the ERG amplitude. Cumulative score and grade severity were both significantly correlated with superficial and deep capillary plexus density (both, $P < 0.001$) in both eyes. Evaluating RORA, we found genes with an overall less severe phenotype, such as *EYS*, *PCDH15*, and *PRPF31*, and those with a worse phenotype, such as *RPGR*.

Conclusions: The correlation of RORA with structural, functional, and genetic assessment in RP disease leads us to consider RORA as a potential biomarker for prediction of disease stage. Multicenter studies are needed to confirm our findings.

Translational Relevance: The morphofunctional and genetic correlations suggest a role for RORA in RP diagnosis and follow-up.

translational vision science & technology

Introduction

Retinitis pigmentosa (RP) consists of a heterogeneous group of inherited diseases characterized by progressive degeneration of retinal photoreceptors. It is the most prevalent inherited retinal dystrophy, causing a significant burden for patients and for healthcare systems alike. Indeed, affecting around 2.5 million persons worldwide and having a prevalence of approximately 1 in 3000 to 4000 individuals,[1,2] RP represents one of the primary causes of blindness in individuals under the age of 60.[3,4] The disease can be syndromic or non-syndromic. Its transmission is autosomal recessive in 50% to 60% of cases and autosomal dominant in 30% to 40% of cases, and X-linked inheritance occurs in 5% to 15% of cases.[5]

The adaptation of new high-throughput DNA sequencing technologies, such as next-generation sequencing (NGS), has expedited the identification of many novel RP-causing genes, but, due to the heterogeneity of the mutations that have been disclosed, establishing the prognosis of the disease remains a great challenge. Depending on the specific gene mutation, the progression rate of the disease can vary. The onset of symptoms occurs in infancy or during adulthood, and the average annual progression (i.e., visual field [VF] loss) is 4% to 12%.[5] Generally, autosomal dominant RP is associated with the best prognosis, whereas X-linked RP is associated with the worst.[3] Standard medical follow-up consists of an annual ophthalmic examination, including visual acuity testing, Goldmann visual field measurements, dilated fundoscopy, optical coherence tomography (OCT), fundus autofluorescence, occasionally fluorescein angiography, and the evaluation of a- and b-wave amplitudes on electroretinograms (ERGs).[6] Fundus alterations include hyper- and hypopigmentated bone spicules, waxy disc pallor, and arteriolar constriction. Also, well-known atypical fundus phenotypes include retinitis punctata albescens. Optic nerve head drusen, cystoid macular edema, vitreous cells, epiretinal membrane, and posterior subcapsular cataract are common signs of panretinal dystrophies. Such complications commonly lead to decreased visual acuity, which is a common symptom together with nyctalopia and reduced VF.

Based on best-corrected visual acuity (BCVA), Goldmann visual field perimetry, and ellipsoid zone (EZ) width (each of which is assigned a score from 0 to 5), Iftikhar et al.[7] recently introduced a new severity staging system for RP, the RP-SSS. Although a residual foveal cone function is often still detectable in the fourth, fifth, and sixth decades of life, the outer nuclear layer thickness and EZ width gradually decrease. Indeed, determining the degree of retinal atrophy involving retinal pigment epithelium (RPE) and photoreceptors in the macular region may be crucial for the visual prognosis and for the evaluation of the efficacy of photoreceptor-rescuing treatments.

The area of focal or large macular central retinal atrophy (CRA) can derive from automatically calculating the area of sub-RPE illumination (SRI) in some OCT devices as previously reported.[8] In fact, some spectral-domain OCT (SD-OCT) software is able to identify SRIs as brilliant areas of increased light transmission beneath the RPE (indicating RPE/outer retina atrophy) and to measure them in an area of 5 mm surrounding the fovea. Based on an international consensus, this technology has already been used in age-related macular degeneration (AMD), where SRI is able to assess the area of retinal pigment epithelium and outer retinal atrophy (RORA).[9] Also, our group has applied this measuring technique in patients with *EYS*-related RP, confirming that it is a valid instrument to correlate severity scores with central retinal atrophy, central visual acuity, and EZ width.[10] This aim of this study was to determine whether in patients with RP there is a correlation among disease severity, morphofunctional parameters, and the extension of RORA, as determined by automated SRI measurements.

Methods

Between March 2020 and December 2022, at the Center for Inherited Retinal Degenerations of the Fondazione Policlinico Universitario Agostino Gemelli IRCCS (Rome, Italy), 38 patients with hereditary and de novo forms of typical RP were enrolled in a cross-sectional study. The study was conducted in accordance with the tenets of the Declaration of Helsinki and approved by the Catholic University/Fondazione Policlinico Universitario Agostino Gemelli IRCCS Institutional Ethics Committee (protocol ID no. 3860). Informed consent was obtained from all subjects involved in the study.

Inclusion criteria were (1) diagnosis of typical RP, (2) sufficient cooperation in psychophysical testing, and (3) media sufficiently clear to allow performing high-speed SD-OCT. Patients with concurrent ocular disorders (e.g., amblyopia, glaucoma) or poor cooperation during psychophysical testing and those with lens opacities resulting in signal strengths less than 8/10 on OCT and OCT angiography (OCTA) were excluded.

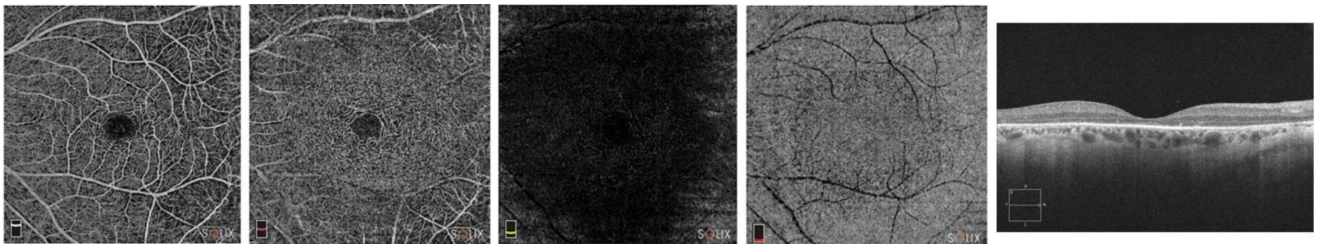

Figure 1. *Left* to *right*, superficial capillary plexus, deep capillary plexus, and outer retina imaging performed with the Optovue Solix OCT and B-scan line performed with the ZEISS CIRRUS HD-OCT 5000 with AngioPlex 10.0 software.

A comprehensive anamnesis, particularly focused on family history, was recorded for each patient in order to identify a genetic patterns or hereditary conditions. All patients underwent a comprehensive ophthalmological examination, including anterior segment biomicroscopy, intraocular pressure measurement, and BCVA (using the Early Treatment Diabetic Retinopathy Study charts). Furthermore, each patient underwent a Goldmann visual field (using the V-4e target), two different SD-OCTs (for measurement of the EZ width), 30-Hz submicrovolt flicker ERG, (Retimax Advanced Plus; CSO, Scandicci, Italy), and direct and indirect ophthalmoscopy. Finally, in accordance with the RP-SSS, the total score for all three variables (ranging from 0 to 15) was used to classify disease severity as grades 0 to 5. The eyes of the participants were evaluated independently (right eye [RE] and left eye [LE]).

Imaging Protocol and Acquired Data

Patients underwent advanced retinal analysis by SD-OCT with the ZEISS CIRRUS 5000 HD-OCT and AngioPlex 10.0 software (Carl Zeiss, Meditec, Dublin, CA) and the Solix OCT (Optovue, Freemont, CA, USA), a new ultra-high-speed spectral domain OCTA device (v1.0.0.317) that operates at 120,000 A-scans per second with the split-spectrum amplitude-decorrelation angiography (SSADA) algorithm. Before image acquisition, 1% tropicamide eyedrops were used to dilate the pupils. A high-definition 5-line raster and a macular map (6 × 6-mm macular cube 512 × 128) were acquired using the ZEISS CIRRUS 5000 HD-OCT AngioPlex, and the Solix OCT scanning protocol included a fovea-centered 6.4 × 6.4-mm field of view. To produce high-density images, a high-definition line (B-scan through the fovea) and a standard multivolume composite (average of four scan volumes) were used as protocol scans. To minimize the impact of circadian variation on the choriocapillaris, the images were captured between 11 AM and 12 PM. The high-definition 5-line raster and 6 × 6-mm macular cube 512 × 128 scan protocols were performed using the CIRRUS HD-OCT 5000 with AngioPlex 10.0 software to evaluate the residual EZ extension and RORA area (Fig. 1).

As previously described,[11] in order to obtain the most reliable measurements, two independent operators (VC, EDA) measured the residual EZ width on horizontal OCT scans using the provided caliper. Particularly, the EZ width was determined using the retinal points where the temporal and nasal EZ borders met the RPE and became indistinguishable. The rate of agreement between the two experts was 92% (95% confidence interval, 81–98). Using the sub-RPE algorithm, the advanced RPE postprocessing analysis then autonomously measured areas of SRI (in mm^2), detecting areas with increased light penetration through the atrophic outer retina, RPE, and choriocapillaris in a 5-mm circular area surrounding the fovea. The SRI is an objective morphological parameter for the evaluation of RORA during the follow-up of eyes with RPE disturbances, as it is able to identify bright areas of increased light transmission below the RPE, indicating RPE atrophy.[12]

The Solix OCT was used to evaluate vascularization centered at the fovea (6.4 × 6.4 mm)—in particular, the superficial capillary plexus, the deep capillary plexus, and the choriocapillaris (Fig. 1). Study participants underwent scanning protocols with a 6.4 × 6.4-mm field of view centered on the fovea. A default internal fixation blue cross light was used to center the scanning area. Two trained operators (MCS, VC) utilized the imaging protocol and, before image processing, worked independently and carefully to visualize all selected images to discern the correctness of the position of the upper and lower boundaries of segmentation corresponding to Bruch's membrane (BM). If segmentation errors were observed, the user manually corrected them on B-scans and then propagated the correction throughout the entire scan volume. All of the choriocapillaris vessel density (VD) evaluations were

performed defining setting the set measurement of the slab between 3 µm above the BR and 30 µm below the BM.

Genetic Testing

Genetic testing was conducted at MAGI's Lab (Rovereto, Italy) and MAGI Euregio (Bolzano-Bozen, Italy). Blood or saliva samples were collected from the study subjects, and DNA extraction was performed using a commercial kit (E.Z.N.A. Blood DNA Kit; Omega Bio-tek, Norcross, GA). The NGS analysis of DNA samples was carried out using a MiSeq DNA sequencer (Illumina, San Diego, CA), in conjunction with an in-house bioinformatics pipeline used for variant calling and annotation, as previously described.[13]

To validate the identified genetic variants, Sanger sequencing was performed using a CEQ 8000 Genetic Analysis System (Beckman Coulter, Milan, Italy). This sequencing method was also employed for family segregation studies when additional family members were available, enabling a more comprehensive understanding of the inheritance patterns of the identified variants.

A comprehensive search for variants was conducted using multiple databases, including the Leiden Open Variation Database (LOVD), dbSNP (https://www.ncbi.nlm.nih.gov/snp/), ClinVar (https://www.ncbi.nlm.nih.gov/clinvar/), and gnomAD (https://gnomad.broadinstitute.org/). The pathogenicity of the identified variants was assessed according to the guidelines set forth by the American College of Medical Genetics and Genomics,[14] with the support of the online tool VarSome (https://varsome.com/).[15,16] Multiplex ligation-dependent probe amplification was used to analyze gene rearrangements for the detection of whole-gene or intragenic rearrangements of specific genes such as *ABCA4*, *EYS*, *RP2*, *PCDH15*, and *USH2A*, following the manufacturer's instructions (MRC Holland, Amsterdam, The Netherlands), and they were analyzed using the Beckman Coulter CEQ 8000 sequencer. Prior to the genetic testing procedure, all patients underwent genetic counseling to gather family history and pedigree information.

Statistical Analysis

The collected data were analyzed descriptively, using frequencies and percentages for categorical data and means and standard deviations (SDs) for continuous data. For inferential statistics, data were considered separately for right and left eyes. Pearson bivariate correlations were performed to check multicollinearity, and Bonferroni correction was applied. Linear regressions were conducted on the clinical variables (retinal AngioVue, BCVA, EZ, VF, cumulative score, grade) to explore the impact on RORA (sub-RPE)/RE and RORA (sub-RPE)/LE. In addition, logistic regressions were conducted on the demographic data to explore the impact of the same outcomes. For this purpose, RORA (sub-RPE)/RE and RORA (sub-RPE)/LE were subsequently coded as binary categorical variables. Statistical significance was set at values of $P < 0.05$. The gene and transmission model available were coded as categorical variables and tested alongside with other clinical variables for a linear regression model using a stepwise forward approach (cut-off $P = 0.2$). Statistical analysis was performed using Stata 17 (Stata Corporation, College Station, TX).

Results

A total of 38 patients (76 eyes) were analyzed. Twenty-three were females (60.53%) and 15 were males (39.47%). The mean age at evaluation was 46.63 ± 15.9 years (range, 16–69), and the average age of onset of symptoms and the mean duration of symptoms were 26.86 ± 19.3 years and 21.73 ± 14.56 years, respectively. Baseline characteristics are reported in the table in the Supplementary Materials. BCVA was 71.05 ± 14.52 letters in the RE and 69.73 ± 16.72 letters in the LE. Mean EZ widths were 7.73 ± 7.13 µm in the RE and 7.516 ± 7.19 µm in the LE. On Goldmann visual field, the mean diameters of the visual fields, in the horizontal meridian using the V-4e stimuli, were 79.31 ± 54.42 mm and 79.02 ± 53.55 mm in the RE and the LE, respectively. Average amplitudes of the fundamental 30-Hz harmonic component derived from submicrovolt ERG were 2.844 ± 5.519 µV in the RE and 2.90 ± 5.55 µV in the LE. The mean RORA sub-RPE measurements were 2.47 ± 4.08 mm^2 and 2.99 ± 4.65 mm^2 in the RE and LE, respectively. The distribution is reported in Figure 2. Using these clinical variables, according to Iftikhar et al.,[7] the disease grading was defined. The average cumulative scores were 7.28 ± 3.64 and 7.44 ± 3.81, respectively, in the RE and LE. The mean grades were 2.84 ± 1.24 (range, 1–5) in the RE and 2.81 ± 1.31 (range 1–5) in the LE.

Results regarding the capillary plexuses are reported in the Supplementary Materials. When assessing the correlations between RORA and the other variables, atrophy correlated well with BCVA (RE $P = 0.04$ and LE $P = 0.005$), EZ (RE $P = 0.005$ and LE $P < 0.001$), and disease severity (RE $P = 0.02$ and LE $P = 0.009$) and grade (RE $P = 0.02$ and LE $P = 0.01$). In contrast,

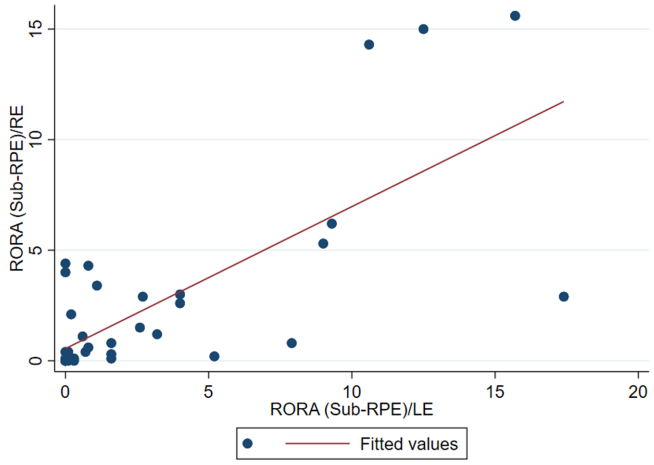

Figure 2. Distribution graph reporting RORA in the RE and LE.

there was no significant correlation with either visual field (RE $P = 0.74$ and LE $P = 0.82$) or amplitude of the first harmonic from the ERG responses (RE $P = 0.72$ and LE $P = 0.68$). Although there always was a correspondence between the two eyes up to this point, the same did not hold true regarding the angiographic evaluation. Indeed, a significant correlation with the deep capillary plexus density (whole) in the RE ($P = 0.03$) was found, but not in the LE, and the opposite was found for the whole choriocapillaris (LE $P = 0.04$ and RE $P > 0.05$). In addition, using a linear regression analysis, a significant correlation between RORA and patient age was observed (RE $P = 0.02$ and LE $P = 0.02$). The mean values of the superficial whole VD, superficial fovea VD, deep whole VD, deep fovea VE, and choriocapillaris VD, both whole and fovea, are reported in the Supplementary Materials with standard deviations and minimum and maximum values.

Finally, when correlating the other variables with each other, a significant correlation was found between BCVA and EZ (RE $P = 0.004$ and LE $P = 0.001$), VF (RE $P = 0.006$ and LE $P = 0.001$), cumulative score (RE $P < 0.001$ and LE $P < 0.001$), grade (RE $P < 0.001$ and LE $P < 0.001$), and superficial and deep capillary plexus vessel density (RE $P < 0.001$, LE $P = 0.005$ and RE $P = 0.02$, LE $P = 0.004$, respectively). EZ on the other hand, correlated well not only with BCVA but also with cumulative score and grade (all $P < 0.001$) and with superficial and deep capillary plexus vessel density (all $P < 0.05$). VF correlated with ERG amplitude (all $P < 0.03$), cumulative score and grade (all $P < 0.001$), and superficial capillary plexus vessel density (all $P < 0.005$). ERG amplitude correlated with cumulative score (all $P < 0.02$), grade (all $P < 0.03$), and deep capillary plexus vessel density (all $P < 0.003$). Finally, the cumulative score correlated significantly with grade (all $P < 0.001$), superficial and deep

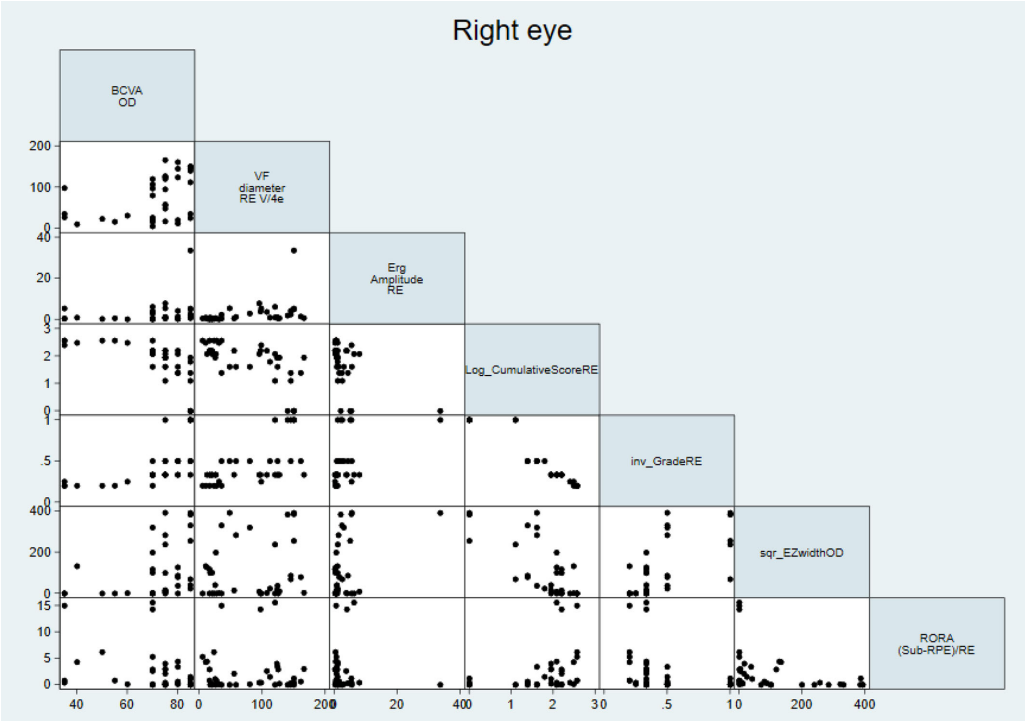

Figure 3. RORA correlation graph with the other variables examined in the RE.

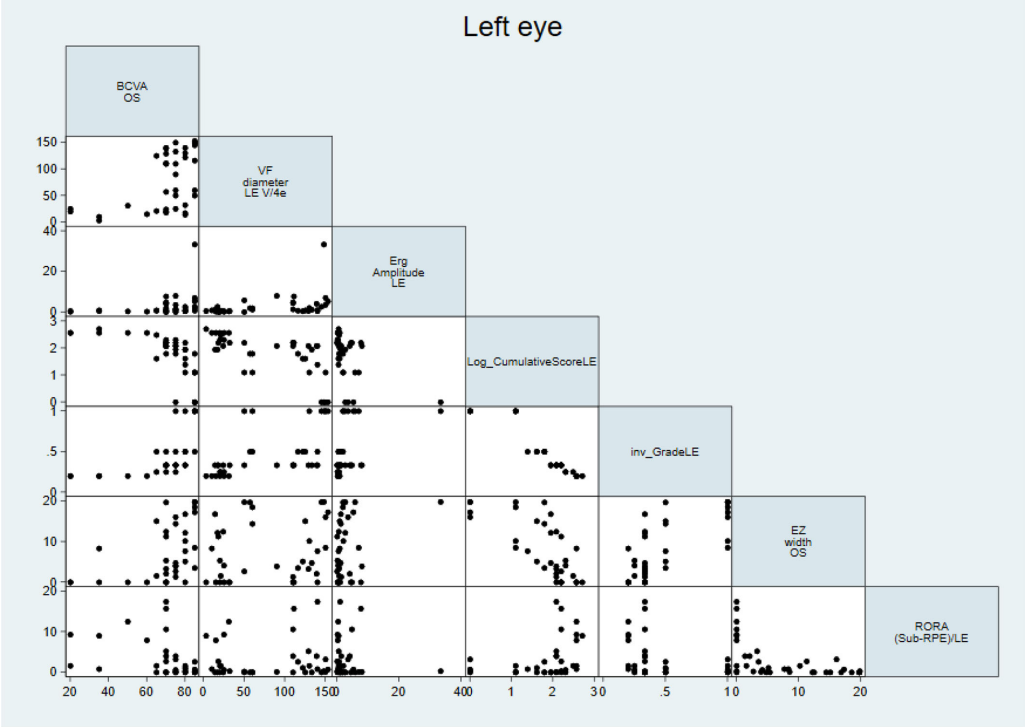

Figure 4. RORA correlation graph with the other variables examined in the LE.

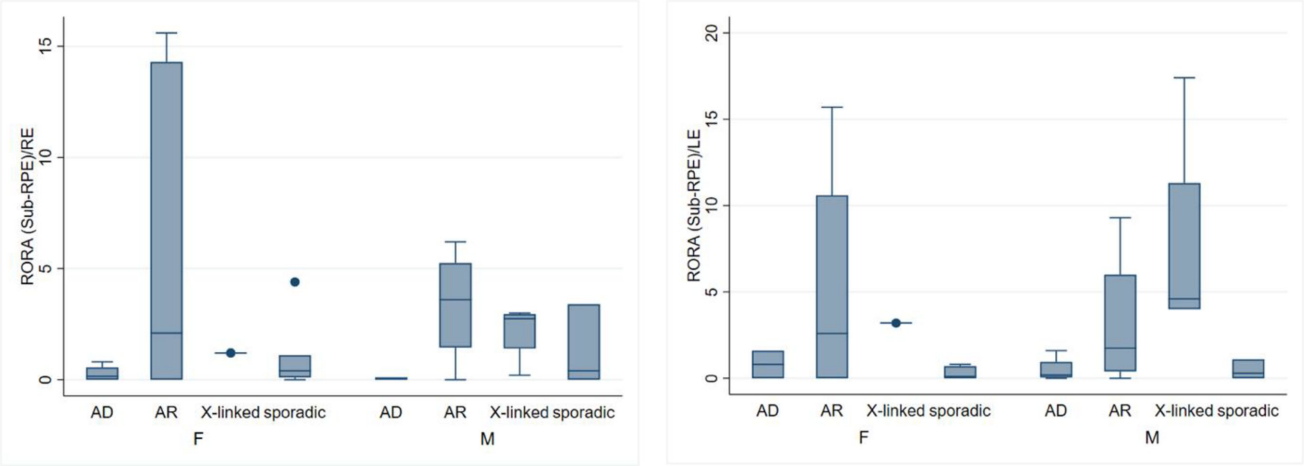

Figure 5. Inherited characteristics correlated with RORA based on sex.

capillary plexus vessel density (both, all $P < 0.001$), and RP disease grade, with superficial and deep capillary plexus density (all $P < 0.002$) only. Figures 3 and 4 show the correlation graphs for RE and LE, respectively.

The studied population was classified according to the inheritance patterns. Evaluating the transmission pattern of the disease, it emerged that eight patients (21%) had an autosomal dominant transmission, 15 patients (40%) had an autosomal recessive transmission, five patients (13%) had an x-linked transmission, and 10 patients (26%) had a sporadic disease occurrence. Inherited characteristics correlated with RORA based on sex are shown in Figure 5.

Genetic mutations were evaluated in the population, and one patient (3%) was positive for an *ADGRV1*[17] mutation, two patients (8%) for an *EYS*[10] mutation, one patient (3%) for a *PCDH15*[18] mutation, one patient (3%) for a *PRPF31*[19] mutation, one patient (3%) for

a *RHO*[20] mutation, one patient (3%) for an *RP1*[21] mutation, and five patients (13%) for an *RPGR*[22] mutation; seven patients (18%) had an initial inconclusive genetic analysis.

In patients whose raw NGS data were evaluable, nucleotide and amino acid variations were also assessed (reported in the Supplementary Materials). For the patients whose genetic analysis was available, a linear regression analysis was performed in order to evaluate correlations with clinical variables, in particular with RORA. Patients with *EYS* mutation ($P = 0.02$), *PCDH15* mutation ($P = 0.05$), or *PRPF31* mutation ($P < 0.001$) were associated with a lower RORA value than the rest of the population and thus had a more favorable clinical picture compared to other patients. A significant relationship between the *RPGR* gene and the LE data was found ($P = 0.001$), indicating that patients with this mutation have a higher RORA and are therefore associated with a more severe disease phenotype than the rest of the evaluated population.

Discussion

Despite being classified as a rare disease, RP significantly impairs the visual abilities of many young patients, affecting not only their social lives but also their education, employment opportunities, and psychological well-being. The purpose of the study was to identify novel progression and prognostic biomarkers of RP, with a particular focus on the role of RORA. As the CAM Study[9] and Müller et al.[24] did in the context of AMD and maternally inherited diabetes and deafness, we evaluated how RORA was correlated with various other parameters in patients with RP.[23] The classification model developed by Iftikhar et al.,[7] which our group recently adapted to the clinical and morphological features of *USH2A*- and *EYS*-related retinal degeneration, is the basis for the current study. Falsini et al.[11] highlighted how *USH2A* severity scores correlate with patient age and with several morphological and functional parameters of retinal disease, and Placidi et al.[10] identified a significant correlation between CRA area and RP-SSS in patients with RP caused by an *EYS* mutation.

The results of our study corroborate the significance of RORA in RP. Its strict correlation with both disease staging (defined as both cumulative score and grade) and patient age demonstrated that changes in this parameter could be considered markers of progression. Furthermore, as previously reported by Savastano et al.[12] and Kiernan et al.[25] in patients with dry AMD, EZ width correlates substantially with both visual acuity and SRI. Similarly, our results demonstrated that RORA could be considered as a marker of disease severity in patients with RP and that its changes go along with angiographic modifications (superficial and deep capillary plexus vessel densities). In line with this result, it could be deduced that the attenuation of retinal vessels, easily observable in patients with retinitis pigmentosa, is relevant to the capillary network as well as the veins and arteries. However, unlike major vessels, capillaries can only be studied with high-resolution techniques capable of detecting microscopic images.

On the other hand, changes in RORA do not seem to have an influence on other angiographic parameters. A larger sample size may be required to achieve statistically significant results. Nonetheless, the evidence of a significant correlation between disease severity and capillary density is of great significance.

Other morphological predicting factors for atrophy progression using OCT analysis have been reported in the literature; however, we focused our attention on RORA because it is the expression of the status of the EZ, outer segments of the photoreceptors, interdigitation zone, and the RPE–BM complex.[26–28] Moreover, as Savastano et al.[8] have already demonstrated in the context of AMD, atrophic areas are simple to study using the quantitative OCT parameter SRI.[29–31]

In addition, we evaluated the genetic characteristics of our population and discovered that disease distribution rates were consistent with those reported in the literature (autosomal dominant RP, 20%–25%; X-linked RP, 10%–15%), with the exception of autosomal recessive transmission, which accounted for 40% of the total in our sample.

This research had several limitations, the most notable ones being the absence of follow-up and the small sample size. As there were only one or two patients for each mutation group, except for the *RPGR* group, these findings cannot be considered definitive. Furthermore, in the advanced stages of the disease, when patients lose their ability to fixate, it is extremely challenging to perform the examinations. Moreover, 50% of patients were unaccounted for the genetic analysis. This inevitably resulted in the exclusion of a subset of patients who could have corroborated our findings.

Conclusions

In conclusion, our finding that a quantitative value, such as SRI, correlates well with other functional

and structural disease variables in patients with RP represents a significant advance in our understanding of the disease. Additionally, the correlations found in this study may be a relevant basis for future evaluation of the efficacy of new therapies. However, in view of the rarity of the disease, multicenter studies would be required to characterize and validate patterns that can predict the disease progression and prognosis.

Acknowledgments

We thank the Ministry of Health for supporting our current research.

Disclosure: **M.C. Savastano**, None; **G. Placidi**, None; **C. Fossataro**, None; **F. Giannuzzi**, None; **N.C. D'Onofrio**, None; **L. Hu**, None; **V. Cestrone**, None; **E. D'Agostino**, None; **I. Biagini**, None; **L. Paris**, None; **G. Coppa**, None; **C. Rizzo**, None; **R. Kilian**, None; **P. Chiurazzi**, None; **M. Bertelli**, None; **P.E. Maltese**, None; **B. Falsini**, None; **S. Rizzo**, None

* MCS and GP contributed equally to this work.

References

1. Campochiaro PA, Mir TA. The mechanism of cone cell death in retinitis pigmentosa. *Prog Retin Eye Res*. 2018;62:24–37.
2. Dias MF, Joo K, Kemp JA, et al. Molecular genetics and emerging therapies for retinitis pigmentosa: Basic research and clinical perspectives. *Prog Retin Eye Res*. 2018;63:107–131.
3. Cross N, van Steen C, Zegaoui Y, Satherley A, Angelillo L. Retinitis pigmentosa: burden of disease and current unmet needs. *Clin Ophthalmol*. 2022;16:1993–2010.
4. Chaumet-Riffaud AE, Chaumet-Riffaud P, Cariou A, et al. Impact of retinitis pigmentosa on quality of life, mental health, and employment among young adults. *Am J Ophthalmol*. 2017;177:169–174.
5. Hartong DT, Berson EL, Dryja TP. Retinitis pigmentosa. *Lancet*. 2006;368(9549):1795–809.
6. American Academy of Ophthalmology. Retinitis pigmentosa: study guide. Available at: https://www.aao.org/Assets/bcc226cb-7ac7-443c-897e-9b20afdfacfb/637153836910470000/r38u-pdf?inline=1&fbclid=IwAR2oP_lD1pWSAROpIfa9poqhZzeSf29_PvZztBZMSQfWKNqTbv1b6t0BXJU. Accessed August 13, 2024.
7. Iftikhar M, Lemus M, Usmani B, et al. Classification of disease severity in retinitis pigmentosa. *Br J Ophthalmol*. 2019;103(11):1595–1599.
8. Savastano MC, Falsini B, Ferrara S, et al. Subretinal pigment epithelium illumination combined with focal electroretinogram and visual acuity for early diagnosis and prognosis of non-exudative age-related macular degeneration: new insights for personalized medicine. *Transl Vis Sci Technol*. 2022;11(1):35.
9. Guymer RH, Rosenfeld PJ, Curcio CA, et al. Incomplete retinal pigment epithelial and outer retinal atrophy in age-related macular degeneration: Classification of Atrophy Meeting Report 4. *Ophthalmology*. 2020;127(3):394–409.
10. Placidi G, Maltese PE, Savastano MC, et al. Retinitis pigmentosa associated with EYS gene mutations: disease severity staging and central retina atrophy. *Diagnostics (Basel)*. 2023;13(5):850.
11. Falsini B, Placidi G, De Siena E, et al. *USH2A*-related retinitis pigmentosa: staging of disease severity and morpho-functional studies. *Diagnostics (Basel)*. 2021;11(2):213.
12. Savastano MC, Falsini B, Cozzupoli GM, et al. Retinal pigment epithelial and outer retinal atrophy in age-related macular degeneration: correlation with macular function. *J Clin Med*. 2020;9(9):2973.
13. Marceddu G, Dallavilla T, Guerri G, Manara E, Chiurazzi P, Bertelli M. PipeMAGI: an integrated and validated workflow for analysis of NGS data for clinical diagnostics. *Eur Rev Med Pharmacol Sci*. 2019;23(15):6753–6765.
14. Richards S, Aziz N, Bale S, et al. Standards and guidelines for the interpretation of sequence variants: a joint consensus recommendation of the American College of Medical Genetics and Genomics and the Association for Molecular Pathology. *Genet Med*. 2015;17(5):405–424.
15. Kopanos C, Tsiolkas V, Kouris A, et al. VarSome: the human genomic variant search engine. *Bioinformatics*. 2019;35(11):1978–1980.
16. Cristofoli F, Sorrentino E, Guerri G, et al. Variant selection and interpretation: an example of modified VarSome classifier of ACMG guidelines in the diagnostic setting. *Genes (Basel)*. 2021;12(12):1885.
17. Fakin A, Bonnet C, Kurtenbach A, et al. Characteristics of retinitis pigmentosa associated with *ADGRV1* and comparison with *USH2A* in patients from a multicentric Usher syndrome study Treatrush. *Int J Mol Sci*. 2021;22(19):10352.

18. Ahmed ZM, Riazuddin S, Bernstein SL, et al. Mutations of the protocadherin gene *PCDH15* cause Usher syndrome type 1F. *Am J Hum Genet*. 2001;69(1):25–34.
19. Wheway G, Douglas A, Baralle D, Guillot E. Mutation spectrum of *PRPF31*, genotype-phenotype correlation in retinitis pigmentosa, and opportunities for therapy. *Exp Eye Res*. 2020;192:107950.
20. Gandra M, Anandula V, Authiappan V, et al. Retinitis pigmentosa: mutation analysis of *RHO*, *PRPF31*, *RP1*, and *IMPDH1* genes in patients from India. *Mol Vis*. 2008;14:1105–1113.
21. Bowne SJ, Daiger SP, Hims MM, et al. Mutations in the *RP1* gene causing autosomal dominant retinitis pigmentosa. *Hum Mol Genet*. 1999;8(11):2121–2128.
22. Zito I, Downes SM, Patel RJ, et al. RPGR mutation associated with retinitis pigmentosa, impaired hearing, and sinorespiratory infections. *J Med Genet*. 2003;40(8):609–615.
23. Sadda SR, Guymer R, Holz FG, et al. Consensus definition for atrophy associated with age-related macular degeneration on OCT: Classification of Atrophy Report 3. *Ophthalmology*. 2018;125(4):537–548.
24. Müller PL, Maloca P, Webster A, Egan C, Tufail A. Structural features associated with the development and progression of RORA secondary to maternally inherited diabetes and deafness. *Am J Ophthalmol*. 2020;218:136–147.
25. Kiernan DF, Zelkha R, Hariprasad SM, Lim JI, Blair MP, Mieler WF. En face spectral-domain optical coherence tomography outer retinal analysis and relation to visual acuity. *Retina*. 2012;32(6):1077–1086.
26. Majander A, Sankila EM, Falck A, et al. Natural history and biomarkers of retinal dystrophy caused by the biallelic *TULP1* variant c.148delG. *Acta Ophthalmol*. 2023;101(2):215–221.
27. Pfau M, von der Emde L, de Sisternes L, et al. Progression of photoreceptor degeneration in geographic atrophy secondary to age-related macular degeneration. *JAMA Ophthalmol*. 2020;138(10):1026–1034.
28. Fleckenstein M, Mitchell P, Freund KB, et al. The progression of geographic atrophy secondary to age-related macular degeneration. *Ophthalmology*. 2018;125(3):369–390.
29. Zhang ZJ, Wu YR, Chien Y, et al. Quantification of microvascular change of retinal degeneration in Royal College of Surgeons rats using high-resolution spectral domain optical coherence tomography angiography. *J Biomed Opt*. 2023;28(10):106001.
30. Duch Hurtado M, Vidal Oliver L, Marín Lambies C, Salom Alonso D. Microvascular quantitative metrics in retinitis pigmentosa using optical coherence tomography angiography. *Arch Soc Esp Oftalmol (Engl Ed)*. 2023;98(5):270–275.
31. Lu B, Chao G, Xie L. Optical coherence tomography angiography in retinitis pigmentosa: a narrative review. *Medicine (Baltimore)*. 2022;101(34):e30068.